AD-A125 750 FINITE WIDTH CURRENTS NON-UNIFORM MAGNETIC SHEAR AND THE CURRENT DRIVEN ION CYCLOTRON INSTABILITY(U) NAVAL RESEARCH LAB WASHINGTON DC P BAKSHI ET AL. 17 MAR 83 1/1

UNCLASSIFIED NRL-MR-5034 F/G 20/7 NL

END

FILMED

DTIC

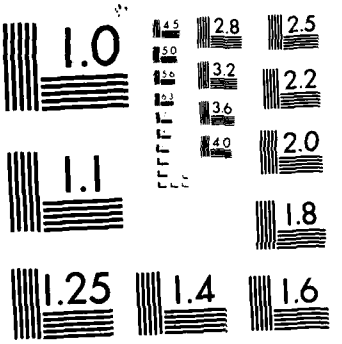

Finite Width Currents, Non-Uniform [illegible] and the Current Driven Ion Cyclotron [illegible]

P. BAKSHI,* G. GANGULI,** AND P. PALMADESSO

Geophysical and Plasma Dynamics Branch
Plasma Physics Division

**Boston College*
Chestnut Hill, MA 02167

***Science Applications Inc.*
McLean, VA 22102

March 17, 1983

This work was supported by the Office of Naval Research and the National Aeronautics and Space Administration.

NAVAL RESEARCH LABORATORY
Washington, D.C.

SECURITY CLASSIFICATION OF THIS PAGE (When Data Entered)

REPORT DOCUMENTATION PAGE		READ INSTRUCTIONS BEFORE COMPLETING FORM
1. REPORT NUMBER NRL Memorandum Report 5034	2. GOVT ACCESSION NO.	3. RECIPIENT'S CATALOG NUMBER
4. TITLE (and Subtitle) FINITE WIDTH CURRENTS, NON-UNIFORM MAGNETIC SHEAR AND THE CURRENT DRIVEN ION CYCLOTRON INSTABILITY		5. TYPE OF REPORT & PERIOD COVERED Interim report on a continuing NRL problem. 6. PERFORMING ORG. REPORT NUMBER
7. AUTHOR(s) P. Bakshi,* G. Ganguli,** and P. Palmadesso		8. CONTRACT OR GRANT NUMBER(s)
9. PERFORMING ORGANIZATION NAME AND ADDRESS Naval Research Laboratory Washington, DC 20375		10. PROGRAM ELEMENT, PROJECT, TASK AREA & WORK UNIT NUMBERS 61153N; RR0330244; 47-0884-0-3; W14365; 266; 47-1447-0-3
11. CONTROLLING OFFICE NAME AND ADDRESS Office of Naval Research NASA 800 North Quincy Street Washington, DC 20546 Arlington, VA 22203		12. REPORT DATE March 17, 1983 13. NUMBER OF PAGES 13
14. MONITORING AGENCY NAME & ADDRESS(if different from Controlling Office)		15. SECURITY CLASS. (of this report) UNCLASSIFIED 15a. DECLASSIFICATION DOWNGRADING SCHEDULE

16. DISTRIBUTION STATEMENT (of this Report)

Approved for public release; distribution unlimited.

17. DISTRIBUTION STATEMENT (of the abstract entered in Block 20, if different from Report)

18. SUPPLEMENTARY NOTES

This work was supported by the Office of Naval Research and the National Aeronautics and Space Administration.

*Present address: Physics Department, Boston College, Chestnut Hill, MA 02167.
**Present address: Science Applications, Inc., McLean, VA 22102.

19. KEY WORDS (Continue on reverse side if necessary and identify by block number)

Electrostatic ion cyclotron waves
Plasma instabilities
Nonlocal effects
Magnetic shear

20. ABSTRACT (Continue on reverse side if necessary and identify by block number)

Our earlier results that non-local effects due to even a small magnetic shear produce a significant reduction of the growth rate of the ion cyclotron instability driven by a uniform current are now generalized to finite width currents. Externally prescribed as well as self-consistent shears are considered. If the current width L_c exceeds the shear length L_s, the previous results are recovered. Shear becomes less effective with reduction of L_c, and for typical parameters, the growth rate attains its (shearless) local value for $L_c L_s \lesssim 10^{-2}$. Non-local effects of the finite current width itself come into play if L_c is further reduced to a few ion Larmor radii and can quench the instability.

DD FORM 1 JAN 73 1473 EDITION OF 1 NOV 65 IS OBSOLETE
S/N 0102-014-6601

SECURITY CLASSIFICATION OF THIS PAGE (When Data Entered)

FINITE WIDTH CURRENTS, NON-UNIFORM MAGNETIC SHEAR AND THE CURRENT DRIVEN ION CYCLOTRON INSTABILITY

In our recent study[1] on the effects of magnetic shear on the current driven ion cyclotron instability (CDICI), we obtained the intriguing result that even a small shear could produce a significant reduction in the growth rate. The transition from the local to the non-local treatment essentially induces a singular perturbation, (the small shear being the coefficient of the highest -- here the second -- derivative term), and there is also a change in the boundary conditions, from plane waves to a bounded solution. It was thus possible to understand and justify the sharp change in the growth rate from the local to the non-local treatment.

However, it was assumed in the treatment above that both the shear and the current were uniform in space. In laboratory as well as space plasmas on the other hand, one necessarily deals with finite width currents, so that the scale length of the current profile is an additional parameter which could play a role in determining the precise nature of the transition from the local to the non-local treatment. One can see, a priori, that if the current width scale length L_c is much larger than the shear length L_s, the effects due to shear should prevail unhindered. In the other limit, when L_c is much smaller than L_s, it is also clear that the total change in the angle of the magnetic field vector in traversing the slab will be so small that the non-local effects due to shear may not come into play, and the local growth rate should prevail, apart from any non-local effects due to the variation of the current profile itself. Thus a transition from the local to the non-local results will occur as the current width is increased from a value much smaller than the shear length to a value larger than the shear length; this transition can be expected to be primarily governed by the ratio of these scale lengths, and a quantitative study of this phenomenon is the main objective of this memo report.

An additional feature to be considered is the relationship between the current profile and the shear. If the shear is entirely generated by the driving current, we will call it the self-consistent shear. If the shear is generated by (stronger) external currents which do not drive the instability, we will call it the prescribed shear. These two cases could lead to slightly different results. Examples of one situation or the other

Manuscript approved January 5, 1983.

can be found in various plasmas of practical importance, and there are also situations where the total shear derives from both the mechanisms.

With the introduction of a finite slab, the problem can no longer be translated to a convenient origin where the given wave vector is perpendicular to the local field line. Instead, we will take the center of the slab as the origin and introduce explicitly $k_{\parallel}^{o}$, the parallel component of the wave vector, as a prescribed parameter. One must maximize over all possible $k_{\parallel}^{o}$, even in the non-local theory, to obtain the optimal normal mode solution. We introduce a finite current width along the x direction by taking the electron distribution function to be a shifted Maxwellian with a drift velocity parallel to the magnetic field to be

$$V_d(x) = V_d^o\, g(x_g/L_c),\ g(\xi) = e^{-\xi^2},\ x_g = x + \frac{v_y}{\Omega_e}\,. \tag{1a}$$

The Vlasov equation is satisfied since x_g, the guiding centre position is a constant of the motion, v_y being the electron velocity component perpendicular to the magnetic field direction z and Ω_e is the electron gyrofrequency. A very small correction in the constant of motion due to shear can be ignored here. The current profile is then found to be

$$j(x) = n_o e V_d^o \exp\left[-x^2/(L_c^2 + \rho_e^2)\right] \approx n_o e V_d^o g(x/L_c), \tag{1b}$$

where $\rho_e^2 \ll L_c^2$ can be ignored; this is also equivalent to replacing x_g by x in equation (1a). This will generate a self-consistent shear in the magnetic field, given in terms of $\xi = \frac{x}{L_c}$ by

$$B_y(x) = \frac{4\pi}{c}\int_o^x j(x)dx = \frac{4\pi n_o e\, V_d^o L_c}{c}\int_o^{\xi} g(\xi)d\xi, \tag{2}$$

$$B_y(x)/B_z = (L_c/L_s)\int_o^{\xi} g(\xi)d\xi,$$

$$(1/s) = L_s = \frac{cB_z}{4\pi n_o e V_d^o}\,, \tag{3}$$

and a corresponding variation of the parallel wavenumber,

$$k_{\parallel}(x) = k_{\parallel}^{o} + k_y B_y(x)/B_z, \tag{4a}$$

or

$$u(x) = k_{\parallel}(x)/k_y = u_o + (L_c/L_s) \int_o^{\xi} g(\xi)d\xi. \tag{4b}$$

The shear length is determined by the physical parameters in eq. (3).

Following, the usual procedure for introducing the non-local effects,[1] we let $k_x \to -(1/i)d/dx$, and assuming that the higher derivative terms are less important, we obtain

$$\left[\rho_i^2 \frac{d^2}{dx^2} + Q(u(x), V_d(x))\right]\phi = 0, \tag{5}$$

or

$$\left[\left(\frac{\rho_i}{L_c}\right)^2 \frac{d^2}{d\xi^2} + Q(u, V_d)\right]\phi = 0,$$

where ρ_i is the ion Larmor radius. Apart from the change in definitions of $k_{\parallel}$, u and V_d, to include the space variation of the current, Q is given by

$$Q = -\rho_i^2 Q_1/A \tag{6}$$

where Q_1 and A are described by eqs. (6) and (7) of Ref. 1. In general, it would be necessary to solve (5) by a numerical method such as the Numerov shooting code technique. The case of pure shear, without any effects due to finite current width ($V_d(x) \equiv V_d^o$), was discussed in Ref. 1 by expanding Q to second order around u_o, the angle of maximum growth in local theory given by $Q(u_o) = 0$. The resulting Weber equation provides a dispersion relation for the determination of the eigenmode frequency. When anharmonic terms become important, the error involved in approximating Q by a quadratic form around u_o will become significant. An improved procedure is to consider an expansion around the (complex) position ξ_1 where the derivative of Q with respect to ξ vanishes,

$$Q'(\omega, \xi_1) = 0. \tag{7}$$

Then the dispersion relation (analogous to eq. (18) of Ref. 1), reduces to

$$Q(\omega, \xi_1) = (2\ell + 1)\,(\rho_i/L_c)\,\left[-\tfrac{1}{2}\,Q''(\omega, \xi_1)\right]^{1/2}, \tag{8}$$

where ℓ is the mode number. Equations (7) and (8) are two complex equations for the simultaneous determination of the complex eigenfrequency ω and the complex angle u_1, corresponding to the complex position ξ_1. We have tested the results obtained from eqs. (7) and (8) against the numerical shooting code solution of eq. (5) in a variety of cases, and the results are in excellent agreement for the eigenfrequencies as well as the solutions for the potential ϕ.

Considering Q(u, v) as a function of two variables u and v, each a function of ξ, the explicit expressions for the derivatives are

$$Q' = (L_c/L_s)g\,Q_u - 2\xi(V_d^o/v_e)Q_v, \tag{9a}$$

$$Q'' = (L_c/L_s)^2 g^2 Q_{uu} - 2(L_c/L_s)\xi g Q_u \tag{9b}$$

$$- 4\,(L_c/L_s)(V_d^o/v_e)\xi g^2 Q_{uv}$$

$$- 2g(1-2\xi^2)(V_d^o/v_e)Q_v + 4(V_d^o/v_e)^2\xi^2 g^2 Q_{vv}.$$

We have solved eqs. (7) and (8) for a range of slab widths $(L_c/\rho_i) = 10$ to 10^7 and shear lengths $(L_s/\rho_i) = 10^2$ to 10^6. The results are displayed for $\ell = 0$ mode in Figures 1-5. The basic transition from the local to the non-local results is evident in Figure 1, which depicts the growth rate in units of ion Larmor frequency, (γ/Ω_i) as a function of the width of the current slab expressed in units of ion Larmor radius, (L_c/ρ_i). Typical parameters are the ion to electron mass ratio $\mu = 1837$, the electron drift to electron thermal velocity ratio $V_d^o/v_e = 0.28$, the ion to electron temperature ratio $\tau = (T_i/T_e) = 0.5$ and the transverse wave number given by $b = (1/2)\,k_y^2\rho_i^2 = 0.6$. Three different shear lengths are represented by $(L_s/\rho_i) = 10^6$, 10^5 and 10^4. In each case, when L_c is sufficiently large, one obtains the non-local growth rate $\gamma/\Omega_i = 0.0127$. Since the shear strengths considered here are all small, we find the same non-local value for γ. For a stronger shear $(\rho_i/L_s) = 10^{-2}$, (not

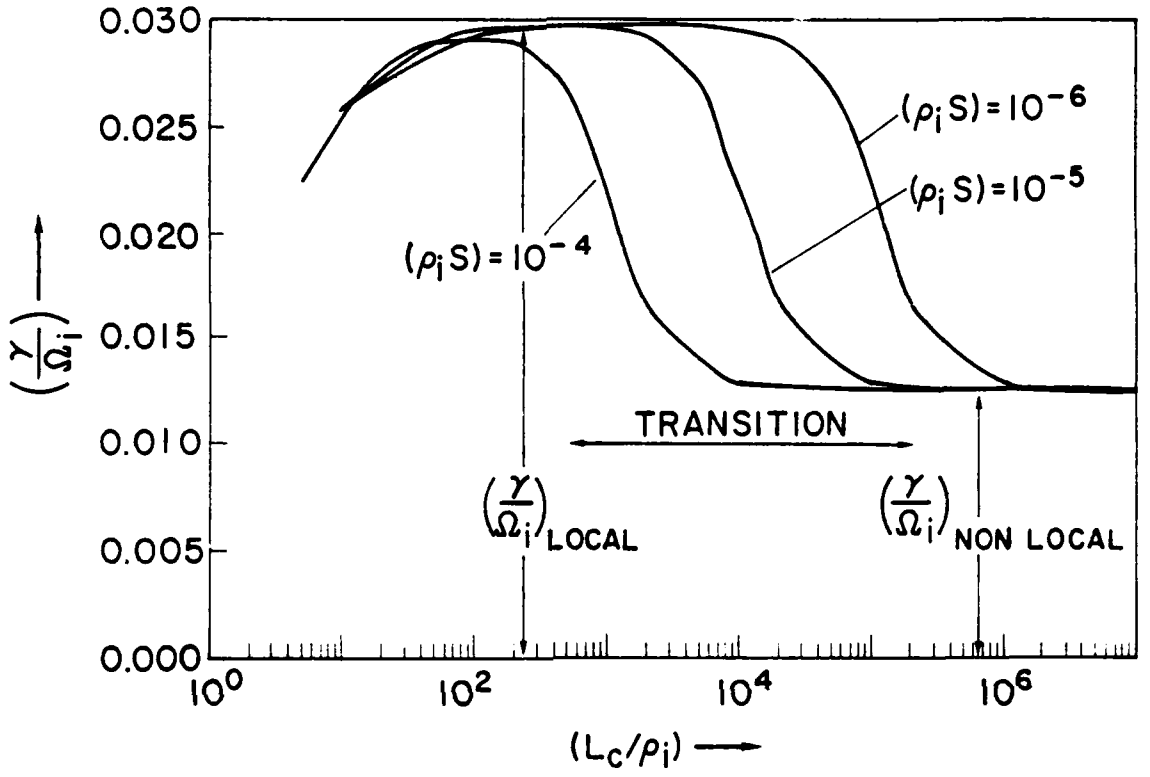

Figure 1 A plot of the growth rate $(\frac{\gamma}{\Omega_i})$ against the current channel width (L_c/ρ_i) for three different magnetic shear lengths. Here $V_d^o = 0.28\ v_e$, $\mu = 1837$, $b = 0.6$, and $\tau = 0.5$.

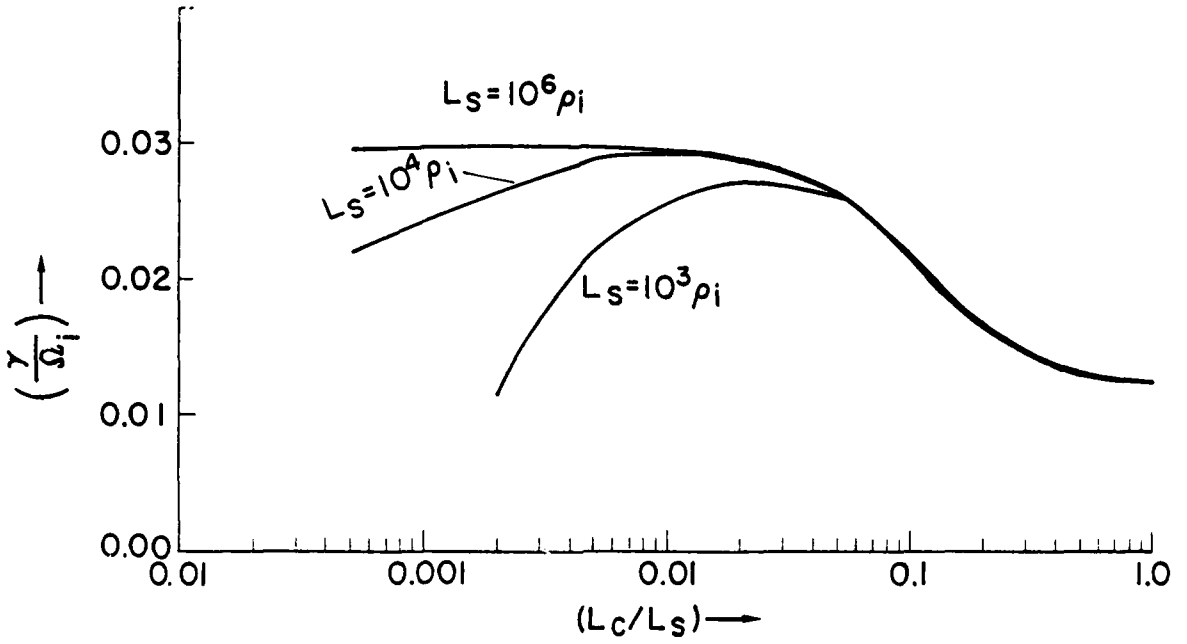

Figure 2a A plot of (γ/Ω_i) against (L_c/L_s) for three different L_s values. Here b = 0.6, μ = 1837, τ = 0.5, and V_d^o = 0.28 v_e. The transition from the local to the nonlocal results are universal, almost independent of the shear value.

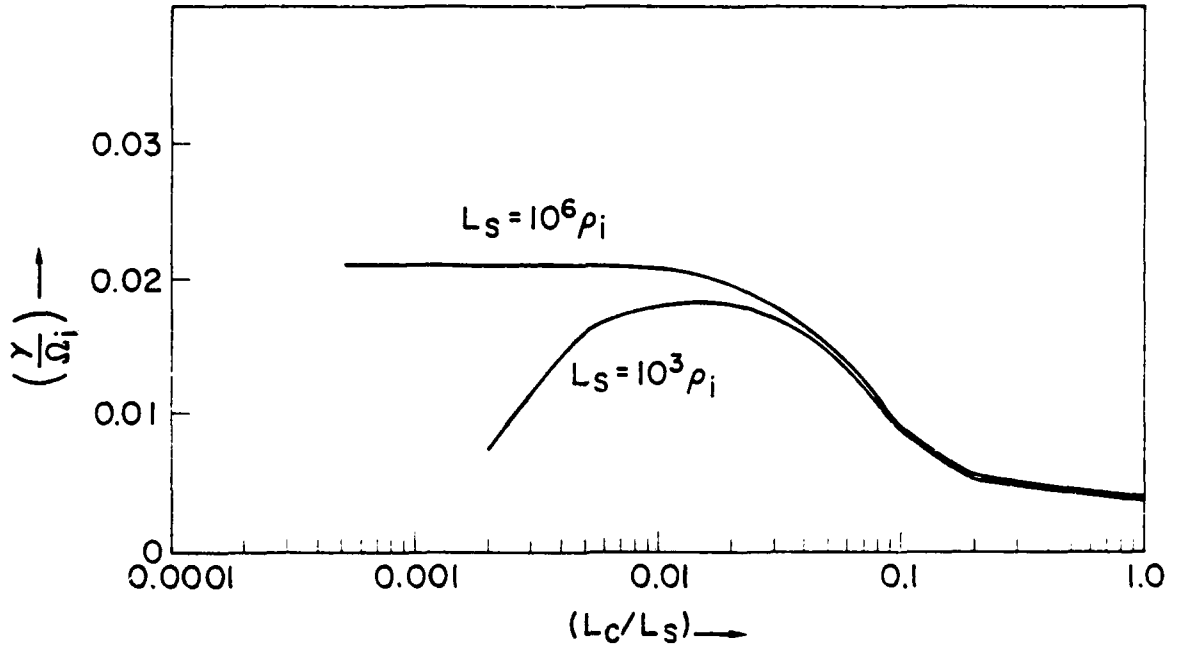

Figure 2b A plot similar to Figure (2a) except that the value of b here is 1.2.

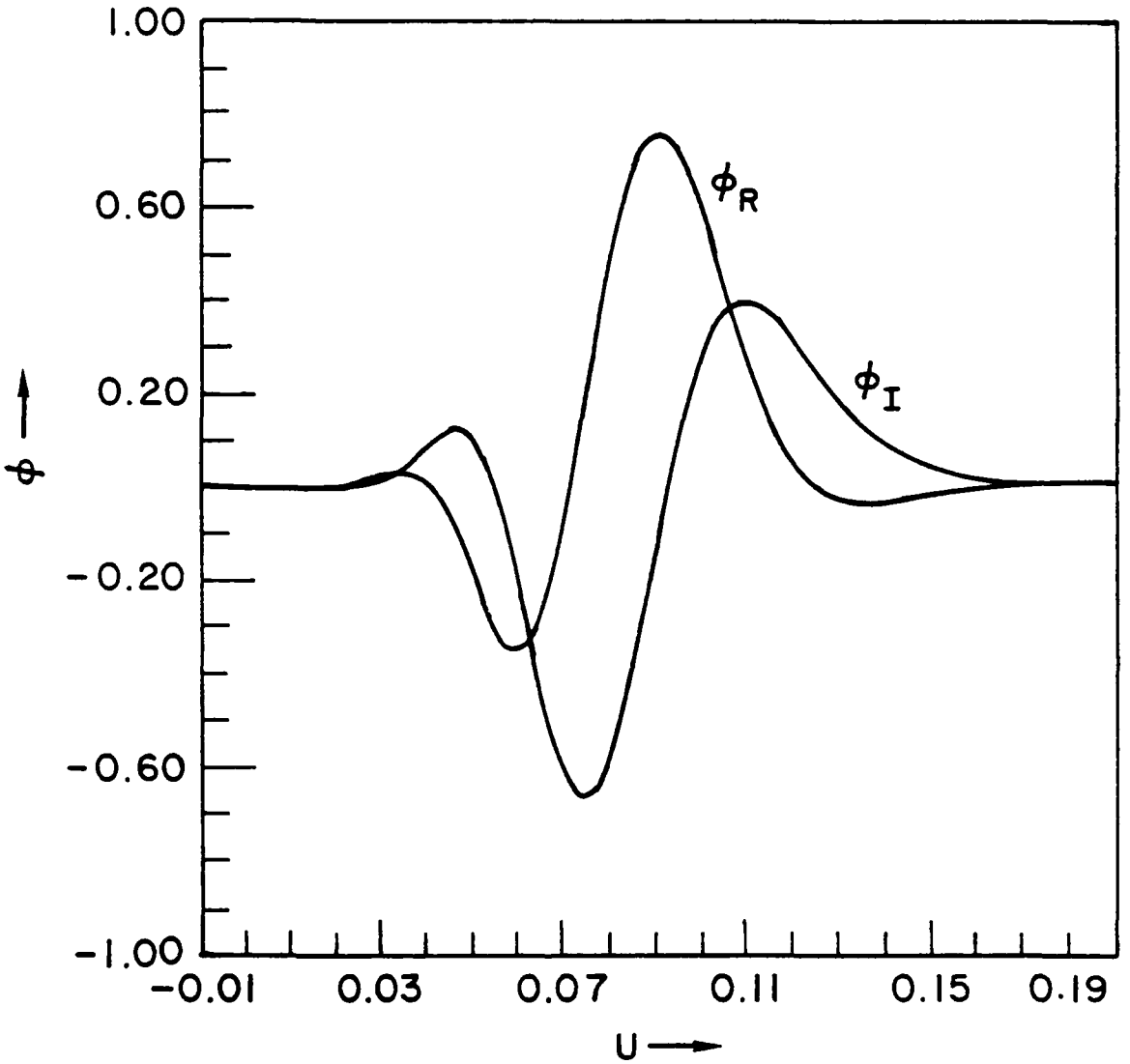

Figure 3 $\phi(u)$ against u for $L_c/\rho_i = \infty$, and $(\rho_i s) = 10^{-2}$, b = 0.6, $V_d^o = 0.28\ v_e$, and $\tau = 0.5$.

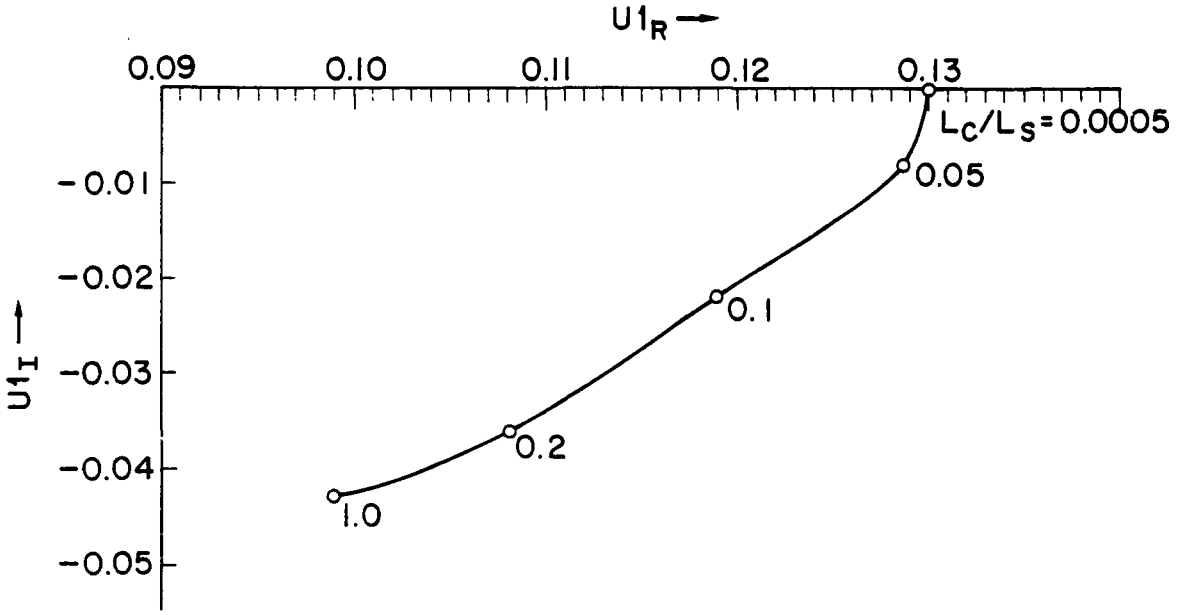

Figure 4a A plot for the complex angle u_1 for various values of L_c/L_s. Here b = 0.6, μ = 1837, V_d^o = 0.28 v_e, and τ = 0.5.

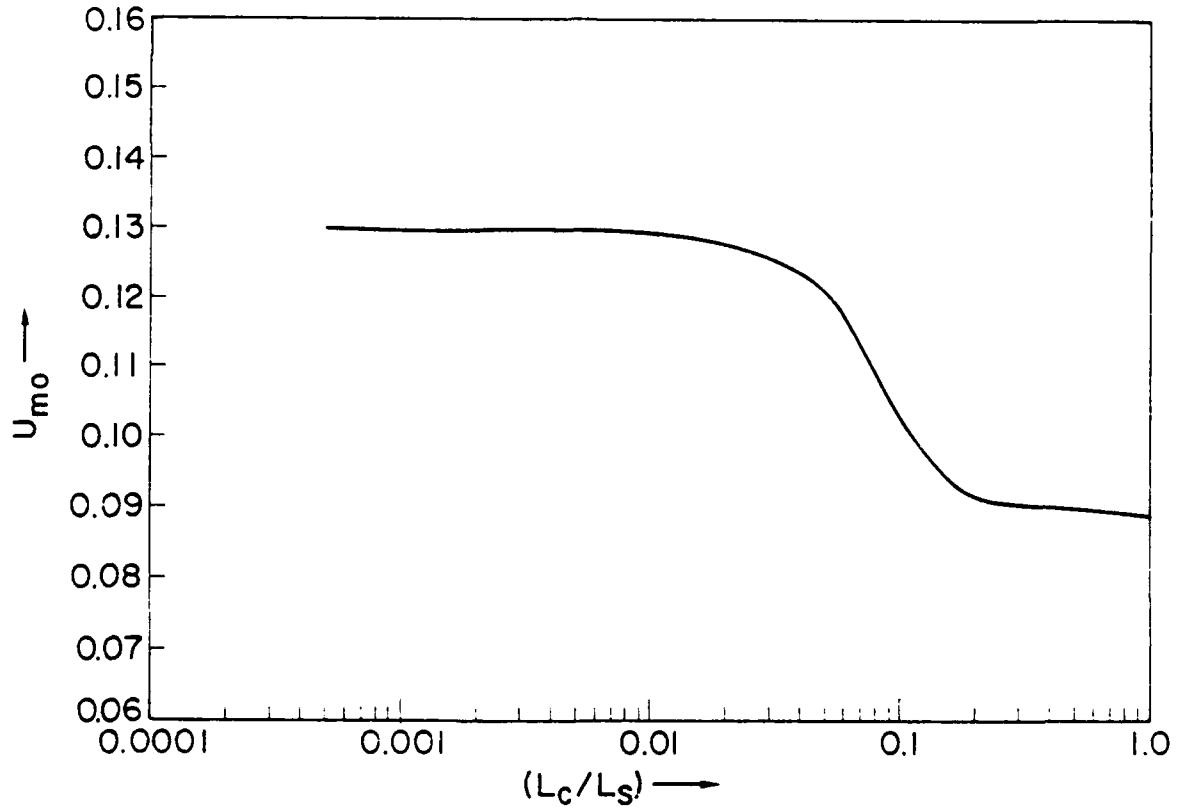

Figure 4b A plot for the real angle U_{mo} where $|\phi(u)|$ attains its maximum, against L_c/L_s. The rest of the parameters are same as Figure 4a.

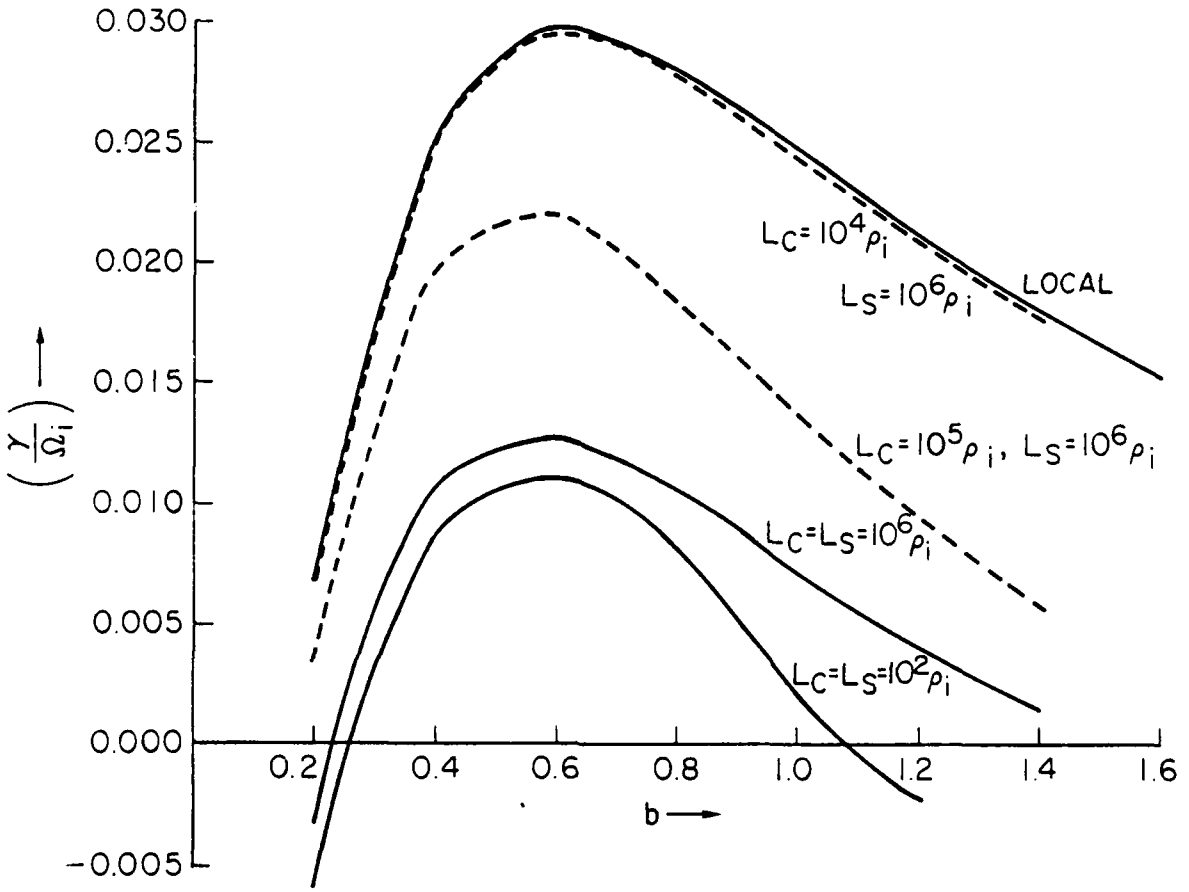

Figure 5 A plot of the growth rates against b. Here $\tau = 0.5$, $\mu = 1837$, $V_d^o = 0.28\ v_e$. The top solid line is a solution of the local dispersion relation. The second solid line is for $L_c = L_s = 10^6 \rho_i$. The dotted lines show the transition from local to nonlocal values as L_c approaches L_s. The lowest solid line is for $L_c = L_s = 10^2 \rho_i$.

shown in Fig. 1), a lower non-local value is obtained, $(\gamma/\Omega_i) = 0.0115$, and still lower non-local growth rates would be attained if the shear is further increased. In the other limit, when L_c is sufficiently small, the local growth rate prevails, $(\gamma/\Omega_i) = 0.0296$. The transition curves for different shear values look very similar, apart from a shift in L_c, and indeed as shown in the next figure, possess a universal behavior as a function of L_c/L_s. Another interesting feature in Fig. 1 is the decrease in growth rate for $L_c < 10^2\rho_i$, which arises from the nonlocal effect of the space variation of the current itself. The slab width is too small to obtain any significant variation of the direction of the magnetic field due to shear, and thus this reduction in growth rate is independent of the shear parameter. If the current width is further reduced to just a few ion Larmor radii, the instability is completely quenched. We can call this the filamental quenching -- current filaments only a few ion Larmor radii in width cannot sustain the instability. This feature may be of practical significance in Q-machine experiments.

Figure 2a represents the same information as in Fig. 1, but now plotted as a function of (L_c/L_s). Now the transition from the local to the non-local result is seen to be universal, almost independent of the shear parameter. Of course, shear values with $(\rho_i/L_s) \gtrsim 10^{-2}$ will lead to lower non-local values with corresponding, slight, departures from the universal transition curve. For small $(L_c/L_s) < 10^{-2}$, the case of very small shear, $\rho_i/L_s = 10^{-6}$, retains the local growth rate for the entire range considered, but the case of larger shear, $\rho_i/L_s = 10^{-3}$, falls in the domain $L_c/\rho_i < 10$ and the growth rate is reduced due to filamental quenching. Figure 2b represents the same parameters, except for $b = 1.2$ and essentially describes the same phenomena as in Fig. 2a. We note that both the local and the non-local limit growth rates are lower than those for $b = 0.6$.

A typical solution for ϕ is given in Figure 3, for the parameters of Fig. 1 in the infinite slab limit, $L_c/\rho_i \to \infty$. The shear parameter is $\rho_i/L_s = 10^{-2}$ and the solutions obtained by the analytical method described here or by a direct numerical solution of the differential equation were found to be identical. The solution is centered around $u_{mo} \approx 0.09$ and has a width of $\Delta u \approx 0.01$. The angular width decreases for lower shear, without

any significant change in the center of $|\phi|$. Figures 4a and 4b respectively represent the variations in u_l, the complex angle around which the wave packet for the electrostatic potential ϕ is formed, and u_{mo} the real angle where $|\phi|$ has its maximum along the real angle axis. The angle u_{mo} is experimentally measurable in the sense of normal mode dominance at that angle as measured from the local magnetic field orientation. For the typical case of b = 0.6, we note the progression of u_l from 0.13 in the local limit to (0.099) - i(0.043) in the non-local (shear dominant) limit and a corresponding transition in u_{mo} from 0.13 to 0.09. These curves are drawn for $\rho_i/L_s = 10^{-6}$, but they represent quite accurately the results for higher shears, because of the universality of the transition.

Figure 5 provides the variation of γ as a function of b for various L_c and L_s combinations. The top curve is the <u>local</u> result obtained directly from Q = 0; this corresponds to the case of a uniform magnetic field (zero shear). If we introduce a small shear $L_s/\rho_i = 10^6$ and a comparable current width $L_c/\rho_i = 10^6$, we essentially reach the shear dominant <u>non-local</u> result discussed in Ref. 1. The transition is shown, with $L_c/\rho_i = 10^5$ and 10^4; the latter case is already good enough to almost approximate the local result. Thus we make the transition from the local to the non-local result as L_c/L_s increases from 10^{-2} to 1. The lowest curve is for $L_c = L_s = 10^2\rho_i$ and the difference from the curve above essentially represents the additional effect of the increased shear.

If we use a prescribed rather than the self-consistent shear, the relation between the angle and the physical distance is simpler,

$$u(x) = u_o + (x/L_s). \qquad (10)$$
$$= u_o + (L_c/L_s)\xi$$

It can be easily seen that (4b) reduces to (10) if ξ remains small, a situation which is valid when $L_c > L_s$, the case when the shear effects dominate. We have also solved eqs. (7) and (8), using eq. (10), and the results do not significantly differ from the case of self-consistent shear.

We have shown in this memo report that the non-local effect of shear is tempered by the finite size of the current slab: (1) For $L_c > L_s$ the

shearing of the magnetic field lines across the length of the slab is sufficient to allow the non-local, singular perturbation effects to take place, and the results of Ref. 1 are recovered; (2) For $L_c < L_s$ on the other hand, the finite slab size is smaller than that needed to provide sufficient angular space to form a parabolic domain for Q_I, the imaginary part of Q, of the type of Fig. 5 of Ref. 1. Thus the shear dominated non-local wave packet formation cannot occur unhindered and for $L_c < 10^{-2}L_s$, the local results are recovered; (3) A new effect occurs for $L_c < 10\ \rho_i$, due to the variation of the current itself; thus filamental currents of only a few ion gyroradii may not produce any instability.

The results obtained here are quite significant for space-plasma applications where small shear and finite width current channels obtain in the auroral arc regions. Implications for various space and laboratory plasmas will be described elsewhere.

Acknowledgements

We wish to thank Dr. J. Finn, Dr. P. Guzdar, Dr. J. Huba and Dr. H. Mitchell for many valuable discussions during the course of this work. One of us (P.B.) would like to thank Dr. S. Ossakow for the kind hospitality of the Naval Research Laboratory where this work was done under the Navy/ASEE Summer Faculty Research Program. The other two authors acknowledge support of this work by the Office of Naval Research and by the National Aeronautics and Space Administration.

References

1. G. Ganguli and P. Bakshi, Phys. Fluids, 25, 1830 (1982).


4-8
DTI